Laminin-α4 and Integrin-Linked Kinase Mutations Cause Human Cardiomyopathy Via Simultaneous Defects in Cardiomyocytes and Endothelial Cells

Ralph Knöll, MD, PhD*; Ruben Postel, MSc*; Jianming Wang, PhD; Ralph Krätzner, PhD;
Gerrit Hennecke, PhD; Andrei M. Vacaru, MSc; Padmanabhan Vakeel, PhD; Cornelia Schubert, MD;
Kenton Murthy; Brinda K. Rana, PhD; Dieter Kube, MD; Gudrun Knöll; Katrin Schäfer, MD;
Takeharu Hayashi, MD, PhD; Torbjorn Holm, MD; Akinori Kimura, MD, PhD;
Nicholas Schork, MD, PhD; Mohammad Reza Toliat, PhD; Peter Nürnberg, MD, PhD;
Heinz-Peter Schultheiss, MD; Wolfgang Schaper, MD, PhD; Jutta Schaper, MD, PhD;
Erik Bos, MSc; Jeroen Den Hertog, PhD; Fredericus J.M. van Eeden, PhD; Peter J. Peters, PhD;
Gerd Hasenfuss, MD, PhD; Kenneth R. Chien, MD, PhD; Jeroen Bakkers, PhD

Background—Extracellular matrix proteins, such as laminins, and endothelial cells are known to influence cardiomyocyte performance; however, the underlying molecular mechanisms remain poorly understood.

Methods and Results—We used a forward genetic screen in zebrafish to identify novel genes required for myocardial function and were able to identify the lost-contact (*loc*) mutant, which encodes a nonsense mutation in the integrin-linked kinase (*ilk*) gene. This *loc/ilk* mutant is associated with a severe defect in cardiomyocytes and endothelial cells that leads to severe myocardial dysfunction. Additional experiments revealed the epistatic regulation between laminin-α4 (Lama4), integrin, and Ilk, which led us to screen for mutations in the human *ILK* and *LAMA4* genes in patients with severe dilated cardiomyopathy. We identified 2 novel amino acid residue–altering mutations (2828C>T [Pro943Leu] and 3217C>T [Arg1073X]) in the integrin-interacting domain of the *LAMA4* gene and 1 mutation (785C>T [Ala262Val]) in the *ILK* gene. Biacore quantitative protein/protein interaction data, which have been used to determine the equilibrium dissociation constants, point to the loss of integrin-binding capacity in case of the Pro943Leu ($K_d=5\pm3$ μmol/L) and Arg1073X LAMA4 ($K_d=1\pm0.2$ μmol/L) mutants compared with the wild-type LAMA4 protein ($K_d=440\pm20$ nmol/L). Additional functional data point to the loss of endothelial cells in affected patients as a direct consequence of the mutant genes, which ultimately leads to heart failure.

Conclusions—This is the first report on mutations in the laminin, integrin, and ILK system in human cardiomyopathy, which has consequences for endothelial cells as well as for cardiomyocytes, thus providing a new genetic basis for dilated cardiomyopathy in humans. (***Circulation***. 2007;116:515-525.)

Key Words: heart failure ■ signal transduction ■ cardiomyopathy ■ endocardium

Dilated cardiomyopathy (DCM) is a syndrome characterized by enlargement of 1 or both ventricles of the heart, accompanied by diminished myocardial contractility.[1] It is estimated that this complex disease has a genetic contribution in at least 30% of all cases (for a review, see Chien[2]). Although ≈25 different genes or loci have been identified,

most of the genes involved encode cardiomyocyte- or myocyte-specific genes, such as sarcomeric, structural, and nuclear membrane proteins or components of calcium metabolism.[3] Therefore, all known disease mechanisms deal with this cell type, and other systems, such as cardiac endothelial cells, have not been considered.

Clinical Perspective p 525

Interactions between cells and their surrounding extracellular matrix are essential for proper execution and regulation of survival, proliferation, cytoskeletal organization, and migration.[4] Furthermore, cell–extracellular matrix contact regulates physiological and pathological processes such as development, differentiation, and metastasis. Laminins are cross-shaped, heterotrimeric, extracellular proteins that consist of 1 α-, 1 β-, and 1 γ-laminin chain. Lama4 is part of laminin 8 and 9, major constituents of basement membranes in the heart and blood vessels. Mice that are deficient for laminin-α4 (Lama4) display endothelial defects, hemorrhages, and dilated vessels, followed by cardiac hypertrophy and heart failure, similar to the lost-contact (loc)/integrin-linked kinase (ILK) phenotype (loc/ilk).[5,6] A pivotal role in the contact between the cell and laminins is mediated by the integrin transmembrane receptors $\alpha3\beta1$, $\alpha6\beta1$, $\alpha6\beta4$, and $\alpha7\beta1$. These classic laminin-binding integrins bind to the laminin globular (LG) 1 (LG1) to LG3 modules of the laminin-α chain (reviewed in Sasaki et al[7]). On the adhesion response of cells to the extracellular matrix, integrin clustering triggers binding of a number of cytoplasmic proteins to their cytoplasmic domain. These multimolecular complexes, termed focal adhesions, allow intensive cross talk between the integrin receptors and downstream signal transduction pathways.[8,9] ILK is a highly conserved serine/threonine protein kinase capable of interacting with the cytoplasmic region of the integrin β_1- and β_3-subunit and is widely expressed, including in endothelial cells, skeletal muscle, and cardiomyocytes.[10] Recently, several binding partners of ILK have been identified, such as PINCH, paxillin, and α-,β-parvin (also known as affixin, reviewed in Legate et al[11]). Paxillin and α-,β-parvin can bind to the C-terminus of ILK, which is important for the connection and reorganization of the actin cytoskeleton, lamellipodia formation, and cell spreading.[12–14] Binding to ILK and complex formation of all these factors are necessary for proper localization of ILK to focal adhesions and suggest the convergence of many regulatory mechanisms at the level of ILK in integrin-mediated signal transduction.[15] ILK-deficient mice die early during embryonic development owing to defects in epiblast polarization with an abnormal distribution of F-actin.[16] Furthermore, in vitro studies suggest that the kinase domain of human ilk is involved in downstream phosphorylation of Akt/PKB on ser473 and of GSK-3β on ser9, revealing a function of ILK in suppressing apoptosis and promoting cell survival.[17]

Methods

Subjects, Polymerase Chain Reaction, and Sequencing

Written informed consent for the study was obtained from all participants, and local ethical committees approved the experimental plan. Polymerase chain reactions were performed in MJ Research Dyad thermal cyclers (Waltham, Mass). Primers were designed to amplify 10 integrin-interacting *LAMA4* exons (GenBank: NT_025741) and the complete coding *ILK* DNA (GenBank: AJ404847 and NM_002290) for sequencing. The human mutations have been annotated with the Human Genome Variation Society (HGVS) nomenclature (see Data Supplement for additional details).

Molecular Modeling

The structures of LAMA4 LG1 wild-type (WT) and LAMA4 LG1 Pro943Leu were created by homologous modeling with the program MODELLER version 6v2.[18] The structure of laminin-α2 LG5 domain with pdb-ID 1qu0 was used as a template. Images were created with the program PyMOL version 0.98 (PyMOL Molecular Graphics System, DeLano Scientific, San Carlos, Calif).

Interaction Analysis

The LAMA4 variants were cloned into the vector pGEX2T (GE Healthcare, Munich, Germany) and expressed as fusion proteins with glutathione S-transferase in *Escherichia coli* DH5a. The variants were extracted from cell lysate with glutathione-agarose beads (Sigma-Aldrich, Munich, Germany). The glutathione S-transferase–LAMA4 fusion proteins were eluted in PBS buffer containing 100 mmol/L reduced L-glutathione (Sigma-Aldrich) and dialyzed overnight at 4°C against PBS buffer. Surface plasmon resonance was performed to analyze the interaction of $\alpha3\beta1$ integrin and LAMA4 variants with a Biacore 2000 system (Biacore, Uppsala, Sweden). Five hundred twenty-five picograms of $\alpha3\beta1$ integrin (Chemicon, Temecula, Calif) was immobilized on a C1 sensor chip (Biacore) by amine coupling according to the manufacturer's instructions. Equimolar amounts of purified recombinant LAMA4 (WT, Arg1073X, and Pro943Leu) were injected to measure the increase in mass by the change of the refractive index on the sensor chip on interaction of LAMA4 with the chip's surface. The resulting curves were evaluated with BIAeval (Biacore) to analyze the differences in binding of the LAMA4 variants. Regeneration was achieved by injections of 0.003% TWEEN (Sigma) and dissociation in running buffer, which was the same buffer used for lama-4 dialysis.

Morpholino Injections

Antisense morpholino oligonucleotides (MOs) were obtained from Gene Tools (Philomath, Ore). The *lama4* MO has been described previously.[19] One nanoliter of morpholino solution was injected in the zebrafish embryo at the 1-cell stage, and embryos were incubated at 28°C until the proper stage for analysis.

Blastomere Transplantation

We injected donors at the 1-cell stage with 2% biotin-dextran and 1% rhodamine-dextran (Molecular Probes, Carlsbad, Calif). At the blastomere stage, we performed reciprocal transplants (WT to ILK, n=4; ILK to WT, n=2) with unidentified progeny of loc$^{+/-}$×loc$^{+/-}$ crosses. We identified mutant embryos among donors and recipients only later, when phenotypes became evident. We processed transplanted specimens for whole-mount staining of coinjected biotin-dextran.

Immunohistochemistry and Quantification of Endothelial Cells

Immunohistochemistry was performed as described previously.[20] Anti-LAMA4 antibodies were provided by Drs Erhard Hohenester and Takako Sasaki. Rabbit anti-human von Willebrand factor antibody was provided by Dako Cytomation (Hamburg, Germany). Endothelial cells were detected with von Willebrand factor immunostaining, counted on 4 to 5 high-power-field magnifications per genotype (ie, control heart tissue [donor heart biopsy] and in the biopsy samples available from the individuals carrying the mutations) and expressed as percentage of total cells (identified by nuclear staining with DAPI).

Cell Attachment Assay

Mutant LAMA4 proteins have been cloned, expressed, and purified according to published procedures,[21] except that we used a Strep tag (IBA, Göttingen, Germany) instead of a His tag. The cell-attachment assay was performed essentially as described previously.[22] Briefly, 96-well plates were coated with 30 μL of WT or mutant LAMA4 protein (0.5 μM) overnight at 4°C. The next day, plates were washed with PBS and blocked with 7.5% bovine serum albumin (in endothelial cell basal medium, PromoCell, Heidelberg, Germany) for 1 hour at 37°C. Human umbilical vein endothelial cells (density 1×10^5 cells/mL) were then seeded onto 96-well plates (100 μL per well) and allowed to adhere for 3 hours at 37°C. Plates were washed twice with PBS and fixed and stained with 0.5% crystal violet in methanol for 2 minutes. After extensive washing, the insoluble dye taken up by the adherent cells was extracted in 0.1 mol/L sodium citrate/100% ethanol (1:1), and the absorbance of the solution was read at 540 nm. Results are expressed as percent of control (WT LAMA4).

In Vitro Kinase Assay

COS1 cells transfected with expression vectors encoding human Flag-tagged ILK or mutants were lysed in cell lysis buffer containing 50 mmol/L HEPES pH 7.5, 150 mmol/L NaCl, 1 mmol/L EGTA, 1.5 mmol/L $MgCl_2$, 1% Triton X-100, and 10% glycerol, 2 mmol/L NaF, 1 mmol/L Na_3VO_4, 1 μg/mL leupeptin, and 1 μg/mL aprotinin. The lysates were incubated with anti-Flag monoclonal antibody M2 (Sigma) for 1 hour at 4°C, and immune complexes were bound to protein A sepharose (Amersham Biosciences) for an additional 1 hour with mixing. The immunoprecipitates were washed extensively with HNTG buffer (20 mmol/L HEPES, 150 mmol/L NaCl, 0.1% Triton X-100, and 10% glycerol). Each immunoprecipitate was divided into 2 equal fractions, 1 of which was immunoblotted with anti-Flag antibody, whereas the other was subjected to kinase assay.

ILK kinase assays were performed in 40 μL of kinase reaction buffer (50 mmol/L HEPES pH 7.0, 10 mmol/L $MnCl_2$, 10 mmol/L $MgCl_2$, 2 mmol/L NaF, 1 mmol/L Na_3VO_4) containing 10 μCi of $[\gamma\text{-}^{32}P]$ATP and 5 μg of myelin basic protein. Reactions were incubated at 30°C for 25 minutes, stopped by the addition of 2X SDS-PAGE sample buffer, and resolved by 12.5% SDS-PAGE. Results were visualized by autoradiography.

Statistical Methods

Differences in cell adhesion between the control (adhesion on WT LAMA4) and test (adhesion on P943L, R1073X, or R1073Q LAMA4) group, respectively, were determined by Student t test for unpaired means. Differences in the percentage of von Willebrand factor–positive cells in biopsy samples from patients (n=4 to 5 sections per group) were also determined with Student t test for unpaired means. Values are expressed as mean±SEM unless otherwise stated. Probability values <0.05 were considered statistically significant.

The authors had full access to and take full responsibility for the integrity of the data. All authors have read and agree to the manuscript as written.

Results

Zebrafish Screen and Analysis of the *Loc* Mutant

A screen for novel genes required for myocardial function resulted in the isolation of several zebrafish mutants (R. Postel and J. Bakkers, unpublished data). One mutant isolated from this screen is the "lost-contact" (*loc*) mutant, its name referring to pronounced cell detachments best observed by blistering of the skin. With 660 *loc* mutant embryos, the *loc* mutation was mapped to chromosome 10 with single sequence length polymorphisms and within 50 kb of the z10910 marker (Figure 1). Sequencing of the coding regions of genes located in the proximity of this region revealed a premature stop codon in the *ilk* gene (*ilk* Y319X; Figure 1). In the *loc*

mutants, no zygotic *ilk* mRNA was detected as assessed by in situ hybridization, which suggests that this mutation destabilizes the transcript that leads to nonsense-mediated decay (Figure 1D).[23] The mutant phenotype could be rescued efficiently by injection of 60 pg of synthetic WT *ilk* mRNA (72% rescue, n=215).

The *loc/ilk* mutant embryos display a variety of severe defects, including blood vessel dilation and ruptures due to thinning of the endothelial wall (Data Supplement Figure II) and a failure of the ventricle to form a proper chamber. To analyze the role of ILK in cardiomyocyte function, we transplanted *loc/ilk* mutant cells into the cardiac-forming region of WT embryos (Figure 2). This procedure had no effect on cardiomyocyte function when WT cells were transplanted to WT embryos; however, *loc/ilk* mutant cardiomyocytes did not incorporate normally into a WT ventricle wall and displayed flattened and elongated cell shapes reminiscent of dilated cardiomyocytes. WT cardiomyocytes transplanted in a *loc/ilk* mutant heart efficiently rescued the aberrant morphology of the ventricular wall (Figures 2C and 2D).

Epigenetic Interaction Between ILK and LAMA4

Because LAMA4 interacts with integrin molecules, especially those presented by endothelial cells, it has important implications for endothelial cell survival,[24] and *Lama4*–deficient mice have recently been shown to develop a defect in endothelial cell viability, followed by cardiac hypertrophy and heart failure.[5,6] Morpholino (MO) knockdown of *Lama4* in zebrafish resulted in cardiac dysfunction and hemorrhages in 35% of the injected embryos (n=74, 6 ng of *Lama4* MO), phenotypes that we also observed in *loc/ilk* mutant embryos. Injection of a low dose (3 ng) of the *lama4* MO in *loc/ilk* heterozygous embryos resulted in severe cardiac dysfunction and hemorrhages (31%, n=59) normally only observed in *loc/ilk* homozygous mutants, which supports a strong genetic interaction between *LAMA4* and *Ilk* (Figure 3).

Human *ILK* and *LAMA4* Mutation Scanning

To determine whether mutations at *ILK* and the integrin-interacting domains of the lama-4 gene (*LAMA4*) are associated with cardiac dysfunction in humans, we sequenced *LAMA4* in 180 white subjects and *ILK* in 192 white subjects with DCM and compared sequencing results with those of a well-characterized white control sample comprising 362 individuals. The control population has also been described in 1 of our previous reports[25]; for *ILK,* we screened 350 control individuals in addition to these 362 individuals (Tables 1 and 2). The size of the present control population (724 chromosomes) enables us to identify genetic variants that are at a frequency of at least 0.1% in the population.[26,27] In the *ILK* gene, we observed 1 nonsynonymous mutation (785C>T [Ala262Val]) in a DCM subject but none in the control group. In *LAMA4*, we identified 10 variants in the 180 DCM subjects (Tables 1 and 3). Of these 10 variants, 6 are unreported in the public databases, such as the National Center for Bioinformatics SNP Database; 4 are nonsynonymous (2828C>T [Pro943Leu], 3218G>A [Arg1073Gln], 3328A>G (Ser1110Gly), and 3335G>C [Arg1112Pro]); 5 are synony-
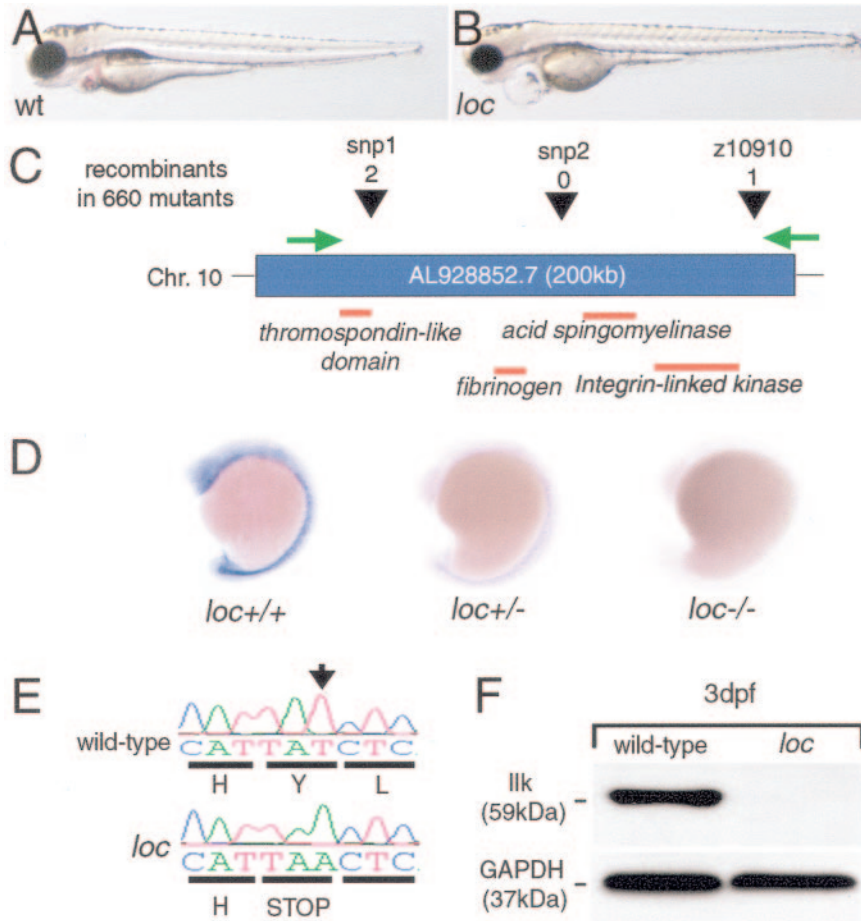
Figure 1. Premature stop codon identified in the *ilk* gene of *loc* mutant embryos. A and B, Morphological comparison between WT sibling embryos (A) and *loc* mutant embryos (B) at 3 days postfertilization. C, Mapping of 660 mutants placed the *loc* mutation on contig Al928852.7 of chromosome (Chr.) 10, between marker z10910 and z6195 (marker not shown). Black arrowheads indicate position of markers used (snp1, snp2, and z10910), and number above it indicates amount of recombinants (out of 660 mutants) for that marker. Open reading frames located on this contig are represented by red lines. D, In situ hybridization with digoxigenin-labeled antisense *ilk* mRNA shows strong *ilk* mRNA expression in homozygous WT ($loc^{+/+}$) embryos, weak expression in heterozygous ($loc^{+/-}$) embryos, and no expression in *loc* mutant ($loc^{-/-}$) embryos at 15-somite stage, which suggests destruction of *ilk* mutant mRNA by the process of nonsense-mediated decay. E, Sequence of exon 10 indicating the T to A mutation found in *loc* mutant embryos, resulting in conversion of a tyrosine (Y), located in the conserved kinase domain at position 319, to a premature stop codon (ILK Y319X). F, Western blot detection of ILK protein in WT sibling embryos and *loc* mutant embryos after 3 days postfertilization (dpf). As a control for the amount of protein in each sample, anti-GAPDH antibody was used.

mous; and 1 variant leads to a premature stop codon (3217C>T [Arg1073X]). We genotyped the control population for these variants and observed the 3218G>A (Arg1073Gln), 3328A>G (Ser1110Gly), and 3335G>C (Arg1112Pro) *LAMA4* single-nucleotide polymorphisms (SNPs), as well as the 5 synonymous SNPs, in equal frequency in the control population. However, the 2828C>T (Pro943Leu) and 3217C>T (Arg1073X) *LAMA4* mutations,
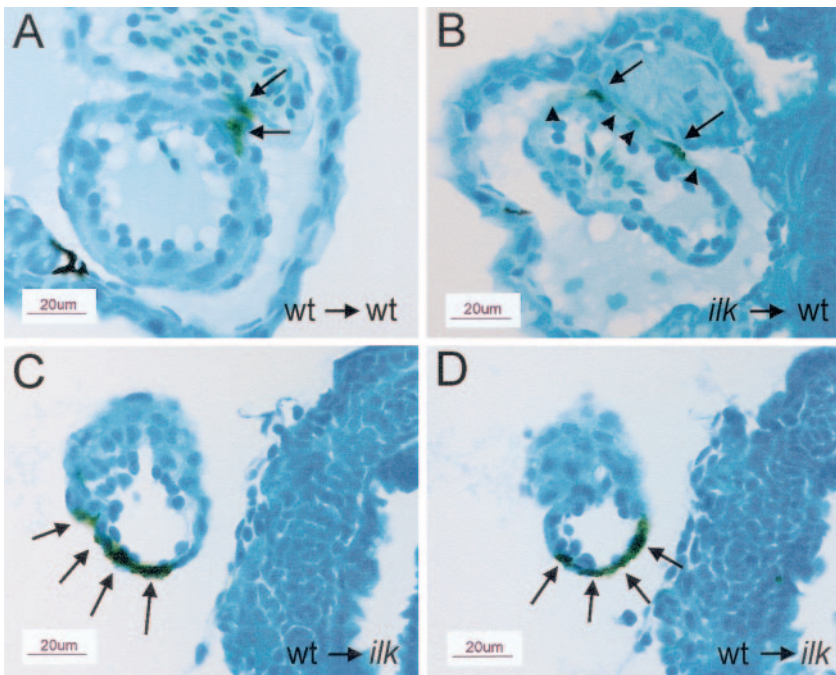

Figure 2. Cell-autonomous effect of ILK on cardiomyocyte cell shape. Mosaic embryos are generated by blastomere transplantation and analyzed at 3 days postfertilization. Transplanted cells are stained brown (biotin labeled) and are indicated by arrows. A, WT cardiomyocytes transplanted into the ventricle of WT embryos have a normal short, thick cardiomyocyte cell shape. B, ILK-deficient cardiomyocytes transplanted into WT hearts display an aberrant flattened and strongly elongated cell shape. Arrowheads point to long, thin cellular protrusions from the 2 transplanted cardiomyocytes. C and D, Two sequential sections of the same embryo. Multiple WT cardiomyocytes transplanted into an ILK-deficient heart form a relatively normal ventricular wall compared with the ventricular wall that is mainly composed of ILK-deficient cardiomyocytes.
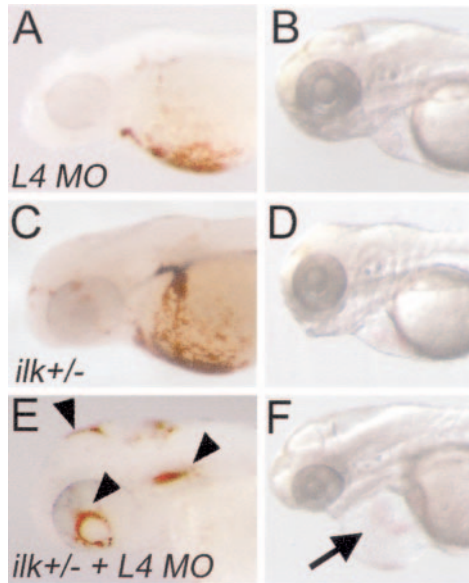
Figure 3. Genetic interaction between *Ilk* and *Lama4*. O-dianisidine hemoglobin blood staining (2.5 days postfertilization; A, C, E) and live photograph (3.5 days postfertilization; B, D, F) of: A and B, WT embryos injected with 3 ng of lama-4 MO showing normal heart morphology and blood within the heart region (52 of 52 embryos); C and D, *loc/ilk* heterozygous embryos showing normal heart morphology and blood within the heart region (49 of 49 embryos); and E and F, 31% of *loc/ilk* heterozygous embryos injected with 3 ng of lama-4 MO displaying hemorrhages in the brain (arrowheads) and cardiac edema (arrow; 18 of 59 embryos, from 3 independent experiments).

identified in white individuals with severe DCM, were not observed in the control population, which indicates that these SNPs may be "private" mutations associated with DCM in the present study subjects. The 785C>T (Ala262Val) *ILK* and the 2828C>T (Pro943Leu) and 3217C>T (Arg1073X) *LAMA4* mutations have been genotyped in an additional 374 DCM patients. Only the 2828C>T (Pro943Leu) *LAMA4* SNP could be found in an additional DCM individual; the 785C>T (Ala262Val) *ILK* and the 3217C>T (Arg1073X) *LAMA4* mutations were not found. Because genetic variation may differ between populations, we also examined a cohort of 200 Japanese individuals for variation at *ILK* and *LAMA4* using SSCP to screen for genetic variants, but no variation was observed (Tables 1 through 3).

Functional Analysis of Human *ILK* and *LAMA4* Mutations

The 785C>T (Ala262Val) *ILK* mutation was found in a proline-rich region of the ILK kinase domain (Figures 4B and

TABLE 1.   Summary of Genetic Variants Found in *LAMA4* Gene

	White Controls	White DCM Individuals
Mutations	0	3*
No mutation	362	551
Total	362	554

*Among whites, we found 1 individual carrying the 3217C>T (Arg1073X) mutation and 2 individuals carrying the 2828C>T (Pro943Leu) *LAMA4* mutations. No mutation was found in an additional 200 Japanese DCM individuals (not included in Table 1).

TABLE 2.   Summary of Genetic Variants Found in Human *ILK* Gene

	White Controls	White DCM Individuals
Mutations	0	1*
No mutation	712	567
Total	712	568

*Among whites, we found 1 individual carrying the 785 C>T (Ala262Val) *ILK* mutation.

4D). To address the effect of this mutation on ILK activity, we performed in vitro binding and kinase assays. Using glutathione S-transferase pull-down assays with recombinant β-parvin and a yeast 2-hybrid system, we observed no differences between WT ILK and ILK A262V in binding to β-parvin (data not shown). We used an in vitro kinase assay to measure ILK kinase activity and compared the result with the previously reported kinase-deficient ILK K220M[12] and with the ILK A262V variant. We observed a 63% reduction in kinase activity for the ILK A262V mutant protein and 80% loss of activity for the ILK K220M variant compared with the WT ILK in this assay (Figure 5A). The 785C>T (Ala262Val) *ILK* mutation has also been analyzed in vivo by injection of synthetic mRNA into *loc/ilk* mutant embryos, which results in high ILK A262V protein levels (Figure 5B). Injection of 80 pg of zebrafish *ilk* A262V mRNA did not cause rescue of the hemorrhages or cardiac dysfunction (0% rescue, n=77), whereas injection of 80 pg of WT *ilk* mRNA did so very efficiently (96% rescue, n=52). Injection of an equal mixture of 20 pg of WT *ilk* mRNA with 20 pg of *ilk* A262V mRNA in *loc/ilk*-deficient embryos also resulted in a poor rescue of the cardiac dysfunction (35% rescue, n=80 compared with 80% rescue for 20 or 40 pg of WT *ilk* mRNA, n=160).

Analysis of the Pro943Leu LAMA4 variant by in silico modeling revealed that this mutation leads to a conformational change of the molecule (Figure 4). The 3217C>T (Arg1073X) mutation deletes 4 of the 5 LG domains at the carboxy terminus of the LAMA4 protein and hence is predicted to impair interaction with integrin molecules. Molecular modeling with the structure of laminin-α2 LG5 used as a template[28] placed Pro943 in a loop of ≈9 amino acids (#942 to #950). To the best of our knowledge, no function has been assigned to any point mutation in this region of LAMA4 LG1 until now. For laminin-α2 LG5, amino acids K3088, K3091, and K3095 were shown to be involved in molecular interaction. In a solid-phase assay, mutations of these residues caused reduced binding to heparin-conjugated albumin and sulfatides or α-dystroglycan.[28] Lys3091 and Lys3095 are located in a turn between 2 β-strands that points to the same direction relative to the β-sandwich of laminin-α2 LG5 as the Pro943-containing loop in LAMA4 LG1 does (Figures 4E and 4F). We therefore assume that this loop region containing amino acids Val942 to Glu950 of LAMA4 LG1 could potentially be involved in molecular interactions.

The substitution of proline 943 to leucine caused a dramatic change in loop conformation predicted by our modeling program. Caused by a flip in the peptide backbone of Pro943Leu, the loop is rotated by roughly 180° (Figure 4F).

TABLE 3.   Summary of Characteristics of Patients Affected by Different *LAMA4* and *ILK* Mutations

Mutation	No. of Patients	Age at Diagnosis, y	Sex	EF, %	Comments
2828C>T (P943L) *LAMA4*	1	53	M	29	...
2828C>T (P943L) *LAMA4*	1	68	M	31	...
3217C>T (R1073X) *LAMA4*	1	29	F	20	Patient prepared for heart transplantation
785 C>T (A262V) *ILK*	1	54	M	25	...

EF indicates ejection fraction.

Note the severe phenotype of the individual affected by the R1073X mutation.

Proteins encoding the LAMA4 Pro943Leu and Arg1073X mutations, the WT protein, and the R1073Q variant (which has been found in unaffected control individuals as well) have been cloned, expressed in vitro, and purified. Adherence of endothelial cells to these different LAMA4 proteins was tested in a cell-attachment assay. Interestingly, LAMA4 Pro943Leu and Arg1073X, but not the R1073Q variant, led to a significant decrease of endothelial cell adherence compared with WT LAMA4–coated wells (Figures 5C and 5D). In addition, the mutant proteins were expressed, purified, and analyzed with a Biacore system, which resulted in demonstration of significantly higher equilibrium dissociation constants for Arg1073X (K_d=1±0.2 μmol/L) and Pro943Leu LAMA4 (K_d=5±3 μmol/L) to immobilized $\alpha3\beta1$ integrin (Biacore) than in the WT LAMA4 protein (K_d=440±20 nmol/L). The differences in binding behavior are depicted in Figure 6, in which the WT protein clearly shows a higher affinity than either mutant at the same concentrations. This might be a possible explanation for the defect seen in the cell-attachment assay (Figure 5).
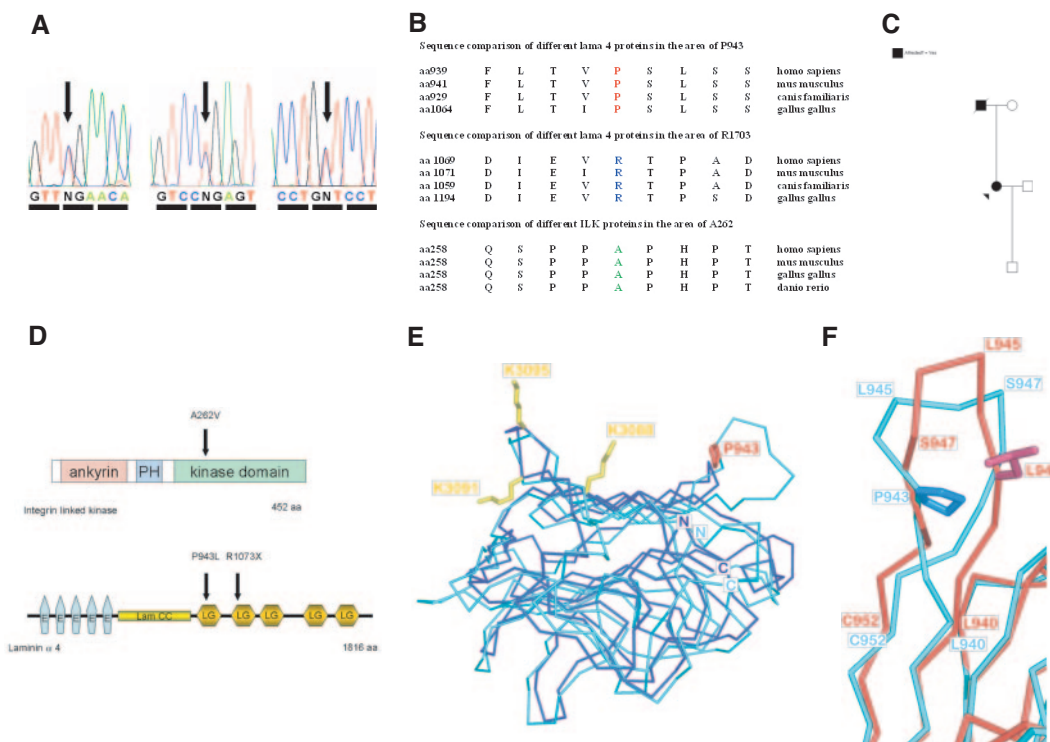

Figure 4. Identification of missense and nonsense mutations in human *ILK* and *LAMA4* genes. A, Sequence chromatograms of the 3217C>T (Arg1073X) mutation (CGA turns into TGA), the 2828C>T (Pro943Leu) mutation (CCG turns into CTG), and the 785C>T (Ala262Val) *ILK* (GCT turns into GTT) mutation. B, Sequence comparison of different *LAMA4* proteins in the areas of the P943 and the R1073 regions, as well as of the A262 ILK region. All 3 amino acids are highly conserved among different species. C, Pedigree of the family of the individual carrying the 3217C>T (Arg1073X) mutation (arrow). Her son does not carry the mutation and is unaffected by the disease, whereas her father is known to have been affected by heart failure. D, Schematic of the ILK and LAMA4 molecules. Arrows indicate human mutations. ILK contains at its amino terminus 4 ankyrin repeat domains and a pleckstrin domain, and at its carboxy terminus, the kinase domain. Lama-4 consists of 5 EGF (epidermal growth factor) repeats, Lam CC (laminin coiled coil), and 5 LamG (laminin-α chain carboxyterminal globular) domains. E, Overlay of the laminin-α2 LG5 domain (dark blue) and the model of LAMA4 LG1 domain (cyan) as ribbons. Lysin residues K3088, K3091, and K3095 (yellow) of laminin-α2 LG5 are involved in molecular interaction. These 3 amino acids are located on the same side of the LG domains' β-sandwich as the loop of LAMA4 LG1, where P943 (red) is located. Amino- and carboxy-termini are labeled as N and C, respectively. F, The predicted loop structures of LAMA4 LG1 WT (cyan) and lama-4 LG1 Pro943Leu (red) are shown as ribbons. The mutation Pro943Leu results in a flip of the peptide backbone. Therefore, the positions L943 (pink) and P943 (blue) are located on opposite parts of the loop with respect to the β-sandwich of the LG domain.
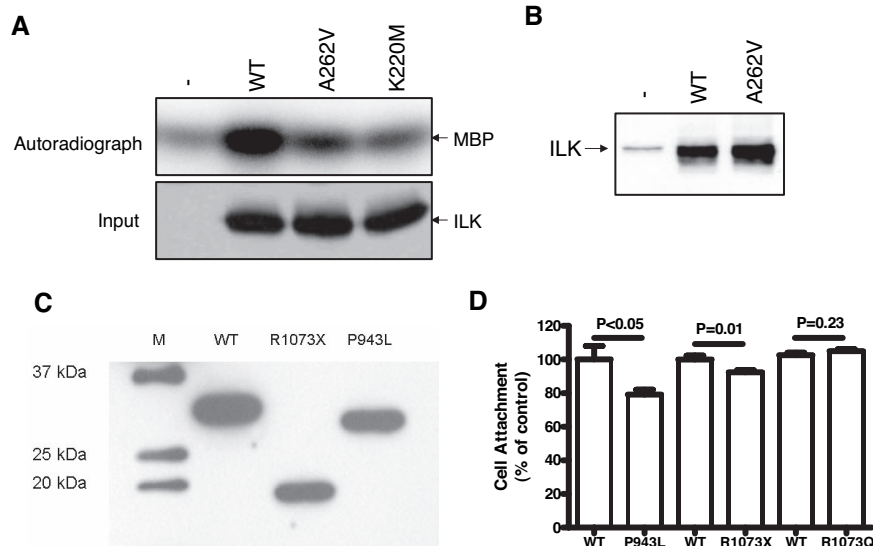
Figure 5. Functional analysis of LAMA-4 and ILK variants. A, Kinase activity of WT, A262V, and K220M ILK proteins. ILK was immunoprecipitated from COS1 cells transfected with empty vector (-), Flag-tagged ILK (WT), or mutants (A262V, K220M). Half of the immunoprecipitate was subjected to an in vitro kinase assay with $[\gamma\text{-}^{32}P]$ATP and myelin basic protein (MBP) as an exogenous substrate. The other half was used for immunoblotting with anti-Flag monoclonal antibody. An autoradiograph (top) and corresponding immunoblot (bottom) are shown. Note the reduction in kinase activity for ILK A262V and for ILK K220M compared with WT ILK kinase activity. B, Expression of WT and A262V ILK after injection of synthetic mRNA in zebrafish embryos. Lane -, no RNA injected, showing endogenous ILK protein. Lane WT, injection of WT *ilk* mRNA. Lane A262V, injection of *ilk* A262V mRNA. Note that only WT *ilk* mRNA injection led to a rescue of the phenotype. C, WT, R1073X, and P943L LAMA4 proteins have been expressed and analyzed by Western blotting after in vitro expression. D, Human umbilical vein endothelial cells were allowed to attach to 96-well plates precoated with WT or mutant (P943L, R1073X, R1073Q) LAMA4 proteins, as described in Methods. The number of adherent cells was examined by measuring the optical density of the extracted dye at 540 nm and is expressed as percent of control (WT LAMA4). Results (mean±SEM) derived from 1 representative experiment are shown.

Furthermore, histological analysis of myocardial biopsy samples points to the loss of endothelial cells in affected patients as the primary cause of cardiomyopathy (Figures 7A and 7B). A detailed quantitative analysis revealed significantly decreased numbers of endothelial cells in patients carrying the 2828C>T (Pro943Leu) *LAMA4* mutation ($P<0.05$; $35.58\pm1.58\%$; n=4), the 3217C>T mutation (Arg1073X; $P<0.002$; $8.25\pm4.8\%$; n=4), or the A262V *ILK*
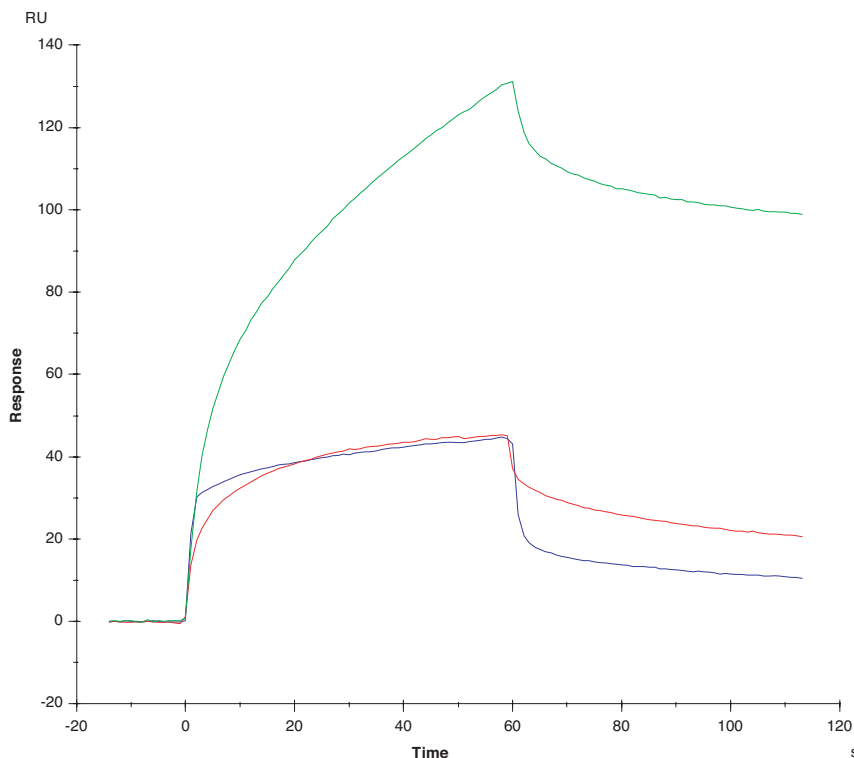
Figure 6. Interaction of LAMA4 variants with immobilized $\alpha3\beta1$ integrin. After immobilization of 450 to 1600 relative units (RU) of $\alpha3\beta1$ integrin on different flow cells of a Biacore C1-sensor chip, 6 μmol/L WT LAMA4, P943L LAMA4, and R1073X LAMA4 were injected on the flow cells. WT LAMA4 (green) was injected into a flow cell with 450 RU of immobilized $\alpha3\beta1$ integrin, P943L LAMA4 (red), and R1073X LAMA4 (blue) to a surface coated with 1300 and 1600 RU, respectively. The resulting increase of mass over time as monitored with surface plasmon resonance was evaluated with BIAeval. Binding curves derived from WT LAMA4 injection show the highest affinity for $\alpha3\beta1$ integrin, whereas P943L LAMA4 and R1073X LAMA4 injections resulted in a distinctly reduced mass increase, which indicates a relative loss of affinity.
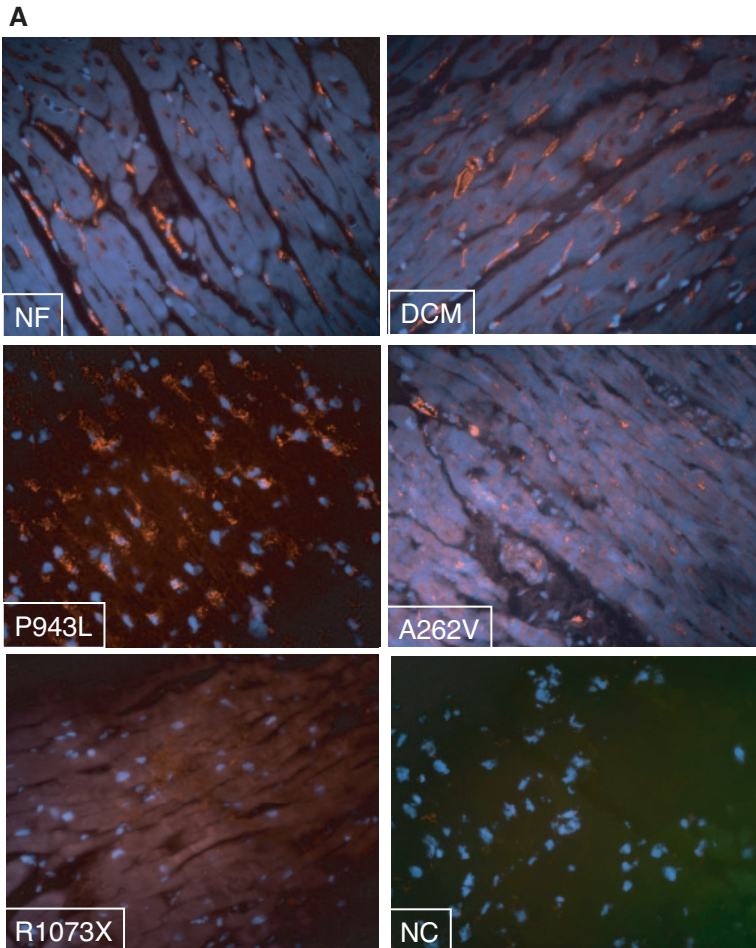
A

Figure 7. A, Immunohistochemistry on myocardial biopsy samples with anti-human von Willebrand factor (vWF) antibodies revealed a significant loss of endothelial cells in individuals carrying the *LAMA4* R1073X or *ILK* A262V mutation, whereas only moderate (but significant) loss of endothelial cells was detected in patients carrying the P943L mutation. NC indicates negative control (first antibody omitted). Biopsy samples from nonfailing myocardium (NF) and patients with DCM are also shown. Red indicates von Willebrand factor–positive endothelial cells; blue, DAPI-positive cell nuclei. Magnification ×400. The results of the quantitative analysis are also shown in panel B.

B
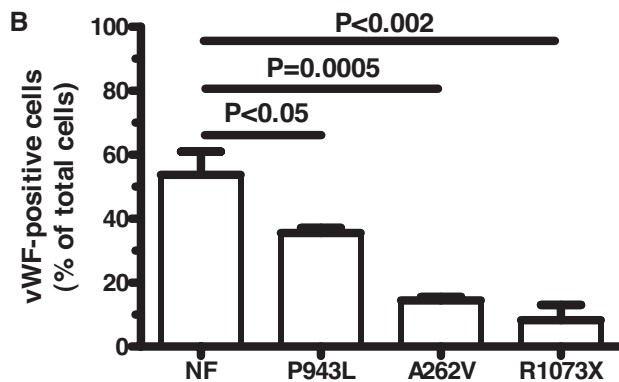
mutation ($P<0.0005$; $14.44\pm1.11\%$; n=5) versus nonfailing control hearts ($53.73\pm7.2\%$; n=4).

Discussion

Here, we report on a novel function for ILK, which is to maintain cardiomyocyte cell shape and morphology of the ventricle during embryonic development, which depends on the presence of the extracellular matrix molecule LAMA4.[29,30] Mice deficient for ILK in cardiomyocytes have no embryonic phenotype, likely owing to the late expression of Cre recombinase under control of the muscle creatine kinase (Mck) promoter.[30] The previously reported zebrafish main-squeeze (*msq/ilk*) mutant, due to a missense mutation in the *ILK* gene (ILK L308P),

affects only cardiac contractility but does not led to development of DCM or any endothelial phenotype.[29,31]

The *loc/ilk* mutant described here develops with a combination of a dysmorphic ventricle with very little ejection during systole and with severe hemorrhages due to thinning and rupture of the endothelial wall. In addition, we show that cardiomyocytes derived from *loc/ilk* mutants and transplanted into a WT heart fail to maintain their compact cell shape and develop thin and stretched cells, resembling human DCM. The apparent differences observed between the previously reported *msq* mutant and the *loc* mutant reported here can be explained by the difference in the type of mutations identified in the *ILK* gene. Although the *msq* mutant harbors a missense
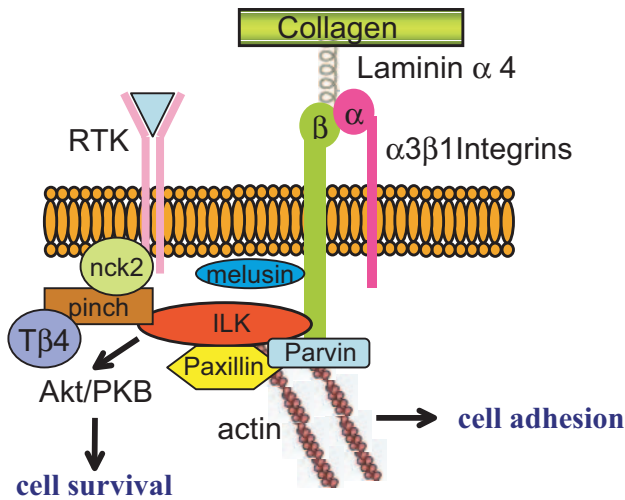
Figure 8. LAMA4 interaction with integrin molecules (especially α3β1 integrins) and its connection with ILK. By controlling AKT kinase activity, as well as by its connection to the cytoskeleton via parvin, the LAMA4–integrin-ILK pathway is central in converting extracellular signals into intracellular survival pathways. Mutations in this system affect endothelial cell and cardiomyocyte survival and lead to cardiomyopathy. RTK indicates receptor tyrosine kinase; Tβ4, thymosin-β4.

mutation (ILK L308P), leaving the rest of the ILK protein intact, the mutation identified in the *loc* mutant is a nonsense mutation within the kinase domain (ILK Y319X). Importantly, the nonsense mutation results in a loss of the mRNA, which prevents any ILK protein from being produced in the *loc* mutants, resulting in a combination of cardiomyocyte and endothelial defects.

The endothelial defects (endothelial wall thinning and ruptures) observed in *loc/ilk* mutant embryos strongly resemble the endothelial defects observed in *LAMA4* knockout mice and are likely due to a loss of interaction between the basement membrane and the actin cytoskeleton, which ultimately results in anoikis (apoptosis initiated on loss of contact with extracellular matrix). Indeed, our genetic experiments in zebrafish demonstrate a linear pathway of LAMA4 with ILK in the developing blood vessel and heart (Figure 8). In myocardial biopsy samples from DCM patients who harbor either the *LAMA4* 3217C>T (Arg1073X) and 2828C>T (Pro943Leu) mutations or the *ILK* 785C>T (Ala262Val) mutation, a very similar combination of a strong reduction in endothelial cells with a cardiomyopathy was observed. This loss of endothelial cells is most likely due to molecular changes in LAMA4 protein structures; either a complete loss of LAMA4 LG2 to LG5 domains, in case of the 3217C>T (Arg1073X) LAMA4, or changes in the loop structure, in case of the 2828C>T (Pro943Leu), which is likely to be involved in molecular interactions and is predicted to change the conformation, may contribute in vitro to the decreased affinity to α3β1 integrins (Figure 6) and in vivo to the defect in endothelial cell attachment (Figure 5).

The 785C>T (Ala262Val) *ILK* mutation, found in an individual with DCM, was unable to rescue the *loc/ilk* phenotype and showed a 63% reduction in the in vitro kinase activity assay, thus pointing to a loss-of-function mutation.

This is in accordance with a recently published report in which *ILK* overexpression was associated with adaptive effects[32] and another report in which *Ilk* deficiency led to heart failure.[30] In addition, it has also been reported recently that ILK improves neovascularization by the recruitment of endothelial progenitor cells during hypoxia.[33] Therefore, the loss of ILK function is also able to explain the loss of endothelial cells in the individual carrying the 785C>T (Ala262Val) *ILK* mutation. The present data on endothelial cells are also in line with the severe, embryonic lethal defect seen in endothelial cell–specific *Ilk* knockout animals.[34] Moreover, ILK has been implicated in cardiac mechanosensation,[29,35] which previously has been shown to be able to affect cardiac function.[20] Therefore, the 785C>T (Ala262Val) *ILK* mutation might also be able to cause heart failure by negatively affecting cardiac mechanosensation, which might be linked to forms of maladaptive hypertrophy.

Interestingly, heterozygous *Ilk* or *Lama4* knockout mice do not develop any known phenotype, which indicates that *Ilk* or *Lama4* haploinsufficiency might not be a disease-causing mechanism in these models.[5,6,10] However, because of their longer life span and thus higher biomechanical stress, humans are at risk of developing heart failure due to more subtle genetic constellations. In addition, the *Ilk* and *Lama4* knockout mice harbor a null allele, whereas patients in the present study harbored either a nonsense mutation (3217C>T [Arg1073X] *LAMA4*) or a missense mutation (2828C>T [Pro943Leu] *LAMA4* or 785C>T [Ala262Val] *ILK*), which might act in a dominant-negative fashion. Moreover, the heterozygous *Ilk*- or *Lama4*–deficient mice have not been challenged by any additional stressors, such as pressure or volume overload, that might be able to unmask a potential phenotype.

In summary, several lines of evidence point to a disease-causing role of mutations within the laminin, integrin, and ILK system (2828C>T [Pro943Leu] *LAMA4*, 3217C>T [Arg1073X] *LAMA4*, and 785C>T [Ala262Val] *ILK*). First, all mutations were located within highly conserved areas of the molecule (Figure 4). Second, all mutations were found in patients affected with severe cardiomyopathy and not in any unaffected individuals. Third, the 2828C>T (Pro943Leu) *LAMA4* mutation is predicted to change the conformation of the molecule. Fourth, the 3217C>T (Arg1073X) *LAMA4* mutation abolishes many of the LG domains of the protein and hence interrupts interaction with integrins. Fifth, *LAMA4* is known to act as a survival factor for endothelial cells,[24] which are found to be severely affected in all carriers of the mutation (Figure 7). Sixth, a recently published *LAMA4*−/− mouse model develops a severe form of cardiomyopathy. Seventh, *lama4* "knock down" in zebrafish and in zebrafish *loc/ilk* heterozygous embryos results in a severe endothelial cell and heart phenotype. Eighth, with the mutant LAMA4 proteins, a significant loss of endothelial cell attachment was observed in the present experiments (Figure 5). Ninth, a mutation in the *ILK* gene (785C>T [Ala262Val]) was also associated with a defect in endothelial cells and heart failure. Injection of synthetic mRNA encoding zebrafish *Ilk* (Ala262Val) into *loc/ilk* mutant embryos cannot rescue the hemorrhages or cardiac dysfunction, whereas injection of WT

ilk mRNA does so very efficiently. Moreover, this mutation is associated with a significant loss of kinase activity. Finally, the flex-chip Biacore system protein interaction analysis points to significant defects in the interaction between mutant LAMA4 and integrin molecules. By disturbing the interaction of endothelial cells and cardiomyocytes with the extracellular matrix, we conclude that mutations located within the laminin-integrin-ILK system may cause cardiomyopathy and heart failure.

Implications

To the best of our knowledge, this is the first systematic screen for mutations in the laminin-integrin-ILK system in cardiomyopathy, and we provide a new genetic basis for this disease in humans (see Figure 8 for a model of the laminin-integrin-ILK system). In addition, endothelial cells may provide a new target for the development of novel cures for DCM. DCM, in contrast to hypertrophic cardiomyopathy (which arises primarily by mutations in sarcomeric genes) might be caused by parallel defects in several cell systems.

Disclosures

None.

References

1. Ahmad F, Seidman JG, Seidman CE. The genetic basis for cardiac remodeling. *Annu Rev Genomics Hum Genet*. 2005;6:185–216.
2. Chien KR. Genotype, phenotype: upstairs, downstairs in the family of cardiomyopathies. *J Clin Invest*. 2003;111:175–178.
3. Seidman JG, Seidman CE. The genetic basis for cardiomyopathy: from mutation identification to mechanistic paradigms. *Cell*. 2001;104:557–567.
4. Giancotti FG, Ruoslahti E. Integrin signaling. *Science*. 1999;285:1028–1032.
5. Thyboll J, Kortesmaa J, Cao R, Soininen R, Wang L, Iivanainen A, Sorokin L, Risling M, Cao Y, Tryggvason K. Deletion of the laminin alpha4 chain leads to impaired microvessel maturation. *Mol Cell Biol*. 2002;22:1194–1202.
6. Wang J, Hoshijima M, Lam J, Zhou Z, Jokiel A, Dalton ND, Hultenby K, Ruiz-Lozano P, Ross J, Tryggvason K, Chien KR. Cardiomyopathy associated with microcirculation dysfunction in laminin alpha 4 chain deficient mice. *J Biol Chem*. 2005;281:213–220.
7. Sasaki T, Fässler R, Hohenester E. Laminin: the crux of basement membrane assembly. *J Cell Biol*. 2004;164:959–963.
8. Nishizaka T, Shi Q, Sheetz MP. Position-dependent linkages of fibronectin- integrin-cytoskeleton. *Proc Natl Acad Sci U S A*. 2000;97:692–697.
9. Choquet D, Felsenfeld DP, Sheetz MP. Extracellular matrix rigidity causes strengthening of integrin-cytoskeleton linkages. *Cell*. 1997;88:39–48.
10. Hannigan GE, Leung-Hagesteijn C, Fitz-Gibbon L, Coppolino MG, Radeva G, Filmus J, Bell JC, Dedhar S. Regulation of cell adhesion and anchorage-dependent growth by a new beta 1-integrin-linked protein kinase. *Nature*. 1996;379:91–96.
11. Legate KR, Montanez E, Kudlacek O, Fassler R. ILK, PINCH and parvin: the tIPP of integrin signalling. *Nat Rev Mol Cell Biol*. 2006;7:20–31.
12. Yamaji S, Suzuki A, Sugiyama Y, Koide Y, Yoshida M, Kanamori H, Mohri H, Ohno S, Ishigatsubo Y. A novel integrin-linked kinase-binding protein, affixin, is involved in the early stage of cell-substrate interaction. *J Cell Biol*. 2001;153:1251–1264.
13. Yamaji S, Suzuki A, Kanamori H, Mishima W, Yoshimi R, Takasaki H, Takabayashi M, Fujimaki K, Fujisawa S, Ohno S, Ishigatsubo Y. Affixin interacts with alpha-actinin and mediates integrin signaling for reorganization of F-actin induced by initial cell-substrate interaction. *J Cell Biol*. 2004;165:539–551.
14. Nikolopoulos SN, Turner CE. Integrin-linked kinase (ILK) binding to paxillin LD1 motif regulates ILK localization to focal adhesions. *J Biol Chem*. 2001;276:23499–23505.
15. Zhang Y, Chen K, Tu Y, Velyvis A, Yang Y, Qin J, Wu C. Assembly of the PINCH-ILK-CH-ILKBP complex precedes and is essential for localization of each component to cell-matrix adhesion sites. *J Cell Sci*. 2002;115(pt 24):4777–4786.
16. Sakai T, Li S, Docheva D, Grashoff C, Sakai K, Kostka G, Braun A, Pfeifer A, Yurchenco PD, Fassler R. Integrin-linked kinase (ILK) is required for polarizing the epiblast, cell adhesion, and controlling actin accumulation. *Genes Dev*. 2003;17:926–940.
17. Delcommenne M, Tan C, Gray V, Rue L, Woodgett J, Dedhar S. Phosphoinositide-3-OH kinase-dependent regulation of glycogen synthase kinase 3 and protein kinase B/AKT by the integrin-linked kinase. *Proc Natl Acad Sci U S A*. 1998;95:11211–11216.
18. Sali A, Blundell T. Comparative protein modelling by satisfaction of spatial restraints. *J Mol Biol*. 1993;234:779–815.
19. Pollard SM, Parsons MJ, Kamei M, Kettleborough RN, Thomas KA, Pham VN, Bae MK, Scott A, Weinstein BM, Stemple D. Essential and overlapping roles for laminin alpha chains in notochord and blood vessel formation. *Dev Biol*. 2006;289:64–76.
20. Knöll R, Hoshijima M, Hoffman HM, Person V, Lorenzen-Schmidt I, Bang ML, Hayashi T, Shiga N, Yasukawa H, Schaper W, McKenna W, Yokoyama M, Schork NJ, Omens JH, McCulloch AD, Kimura A, Gregorio CC, Poller W, Schaper J, Schultheiss HP, Chien KR. The cardiac mechanical stretch sensor machinery involves a Z disc complex that is defective in a subset of human dilated cardiomyopathy. *Cell*. 2002;111:943–955.
21. Gonzales AM, Gonzales M, Herron GS, Nagavarapu U, Hopkinson SB, Tsuruta D, Jones JC. Complex interactions between the laminin alpha 4 subunit and integrins regulate endothelial cell behavior in vitro and angiogenesis in vivo. *Proc Natl Acad Sci U S A*. 2002;99:16075–16080.
22. Hecke A, Brooks H, Meryet-Figuiere M, Minne S, Konstantinides S, Hasenfuss G, Lebleu B, Schafer K. Successful silencing of plasminogen activator inhibitor-1 in human vascular endothelial cells using small interfering RNA. *Thromb Haemost*. 2006;95:857–864.
23. Nagy E, Maquat LE. A rule for termination-codon position within intron-containing genes: when nonsense affects RNA abundance. *Trends Biochem Sci*. 1998;23:198–199.
24. DeHahn KC, Gonzales M, Gonzales AM, Hopkinson SB, Chandel NS, Brunelle JK, Jones JC. The alpha4 laminin subunit regulates endothelial cell survival. *Exp Cell Res*. 2004;294:281–289.
25. Wojnowski L, Kulle B, Schirmer M, Schluter G, Schmidt A, Rosenberger A, Vonhof S, Bickeboller H, Toliat MR, Suk EK, Tzvetkov M, Kruger A, Seifert S, Kloess M, Hahn H, Loeffler M, Nurnberg P, Pfreundschuh M, Trumper L, Brockmoller J, Hasenfuss G. NAD(P)H oxidase and multidrug resistance protein genetic polymorphisms are associated with doxorubicin-induced cardiotoxicity. *Circulation*. 2005;112:3754–3762.
26. Mitchell AA, Chakravarti A, Cutler DJ. On the probability that a novel variant is a disease-causing mutation. *Genome Res*. 2006;15:960–966.
27. Eberle MA, Kruglyak L. An analysis of strategies for discovery of single-nucleotide polymorphisms. *Genet Epidemiol*. 2000;19(suppl 1):S29–S35.
28. Hohenester E, Tisi D, Talts JF, Timpl R. The crystal structure of a laminin G-like module reveals the molecular basis of alpha-dystroglycan binding to laminins, perlecan, and agrin. *Mol Cell*. 1999;4:783–792.
29. Bendig G, Grimmler M, Huttner IG, Wessels G, Dahme T, Just S, Trano N, Katus HA, Fishman MC, Rottbauer W. Integrin-linked kinase, a novel component of the cardiac mechanical stretch sensor, controls contractility in the zebrafish heart. *Gen Dev*. 2006;20:2361–2372.

30. White DE, Coutu P, Shi YF, Tardif JC, Nattel S, St-Arnaud R, Dedhar S, Muller WJ. Targeted ablation of ILK from the murine heart results in dilated cardiomyopathy and spontaneous heart failure. *Gen Dev*. 2006; 20:2355–2360.

31. Stainier DY, Fouquet B, Chen JN, Warren KS, Weinstein BM, Meiler SE, Mohideen MA, Neuhauss SC, Solnica-Krezel L, Schier AF, Zwartkruis F, Stemple DL, Malicki J, Driever W, Fishman MC. Mutations affecting the formation and function of the cardiovascular system in the zebrafish embryo. *Development*. 1996;123:285–292.

32. Lu H, Fedak PW, Dai X, Du C, Zhou YQ, Henkelman M, Mongroo PS, Lau A, Yamabi H, Hinek A, Husain M, Hannigan G, Coles JG. Integrin-linked kinase expression is elevated in human cardiac hypertrophy and induces hypertrophy in transgenic mice. *Circulation*. 2006;114:2271–2279.

33. Lee SP, Youn SW, Cho HJ, Li L, Kim TY, Yook HS, Chung JW, Hur J, Yoon CH, Park KW, Oh BH, Park YB, Kim HS. Integrin-linked kinase, a hypoxia-responsive molecule, controls postnatal vasculogenesis by recruitment of endothelial progenitor cells to ischemic tissue. *Circulation*. 2006;114:150–159.

34. Friedrich EB, Liu E, Sinha S, Cook S, Milstone DS, MacRae CA, Mariotti M, Kuhlencordt PJ, Force T, Rosenzweig A, St-Arnaud R, Dedhar S, Gerszten RE. Integrin-linked kinase regulates endothelial cell survival and vascular development. *Mol Cell Biol*. 2004;24:8134–8144.

35. Srivastava D, Yu S. Stretching to meet needs: integrin-linked kinase and the cardiac pump. *Genes Dev*. 2006;20:2327–2331.

CLINICAL PERSPECTIVE

Dilated cardiomyopathy is a syndrome characterized by remodeling (enlargement) of 1 or both ventricles and diminished myocardial contractile function. Although a variety of pathophysiological mechanisms have been identified in cardiomyocytes, little attention has been given to the possibility that defects in endothelial cells might also play an important role in causing dilated cardiomyopathy. The present report describes the discovery of the first human mutations in the laminin-α4 and integrin-linked kinase genes and how these mutations affect the laminin-α4 integrin–integrin-linked kinase pathway in both cardiomyocytes and endothelial cells. These data suggest a mechanism by which genetic abnormalities in endothelial cells may contribute to the pathophysiology of dilated cardiomyopathy and thereby raise the possibility that new therapeutic options directed at the endothelial cell could be beneficial in dilated cardiomyopathy.

Circulation

Laminin-α4 and Integrin-Linked Kinase Mutations Cause Human Cardiomyopathy Via Simultaneous Defects in Cardiomyocytes and Endothelial Cells

Ralph Knöll, Ruben Postel, Jianming Wang, Ralph Krätzner, Gerrit Hennecke, Andrei M. Vacaru, Padmanabhan Vakeel, Cornelia Schubert, Kenton Murthy, Brinda K. Rana, Dieter Kube, Gudrun Knöll, Katrin Schäfer, Takeharu Hayashi, Torbjorn Holm, Akinori Kimura, Nicholas Schork, Mohammad Reza Toliat, Peter Nürnberg, Heinz-Peter Schultheiss, Wolfgang Schaper, Jutta Schaper, Erik Bos, Jeroen Den Hertog, Fredericus J.M. van Eeden, Peter J. Peters, Gerd Hasenfuss, Kenneth R. Chien and Jeroen Bakkers

The online version of this article, along with updated information and services, is located on the
World Wide Web at:
http://circ.ahajournals.org/content/116/5/515

Data Supplement (unedited) at:
http://circ.ahajournals.org/content/suppl/2007/07/16/CIRCULATIONAHA.107.689984.DC1